Proceedings World Geothermal Congress 2026
Calgary, Canada, June 8 – 11, 2026

Groundwater Heat Pump and Free Cooling Systems for Urban Heat Island Mitigation: A Case Study in the City of Québec, Canada

Victoria Lee[1], Jasmin Raymond[1*], Christine Rivard[2], Félix-Antoine Comeau[1] and Juliet Newson[3]
Institut national de la recherche scientifique, 490 rue de la Couronne, Québec, QC, G1K 9A9, Canada[1*],
Commission géologique du Canada, 490 rue de la Couronne, Québec, QC, G1K 9A9, Canada
Reykjavik University, Menntavegur 1, 101 Reykjavík, Island
jasmin.raymond@inrs.ca

Keywords: Geothermal, Cooling, Aquifer, Open-loop, Heat Wave, Thermal Energy Storage, Numerical Model

ABSTRACT

This study explored the potential of open-loop geothermal systems, specifically groundwater heat pumps (GWHP) and aquifer thermal energy storage (ATES), to replace conventional air-conditioning, which releases heat into the atmosphere. While these systems have the potential to reduce the urban heat island (UHI) effect, the benefits of free cooling without a heat pump remain unevaluated. The objective of this study was to assess the performance and thermal impact of geothermal cooling solutions in mitigating UHIs. For this, we selected a sandy aquifer located beneath Quebec City (Quebec, Canada), which experiences UHI effects, like many other cities in Canada. Fieldwork was conducted, including the drilling of pumping, injection and observation wells in which different field tests were performed. Numerical models were developed with FEFLOW to simulate various scenarios comparing GWHP and ATES systems, both with and without free cooling, over their operation lifetime (25 years). Results indicate that ATES systems slightly outperform GWHPs, benefiting from better abstraction temperatures because of the stored thermal energy. Both systems performed significantly better during cooling than heating periods. Moreover, 100% free cooling achieved a high seasonal performance factor of 19.13, while maintaining a solid performance in heating mode. Its thermal impact on the aquifer was lower than that of heat pump-based scenarios, highlighting the potential of free cooling to improve efficiency while minimizing subsurface disturbances. These findings offer valuable guidance for decision makers seeking sustainable cooling (and heating) strategies, particularly in regions with similar hydrogeology and a cold humid continental climate.

1 INTRODUCTION

Urban heat islands (UHIs) have become a growing concern in large Canadian cities. Such UHIs result from extreme summer temperatures caused by climate change and are exacerbated by increased urbanization, leading to higher temperatures in densely populated areas compared to their rural surroundings. The intensification of UHIs can have detrimental effects on human health and well-being, as well as energy consumption (Vujovic et al. 2021). Conventional air conditioners contribute to this phenomenon (up to 2°C) due to the heat rejected into the ambient air (Salamanca et al. 2014). It consequently appears relevant to explore low-carbon cooling methods as alternative solutions to mitigate the intensity of UHIs and their impacts.

Geothermal systems offer a promising alternative to conventional air conditioning systems. Open-loop systems, such as groundwater heat pumps (GWHP) and aquifer thermal energy storage (ATES) systems, have the potential to significantly reduce energy consumption. Indeed, the amount of heat released into the air and greenhouse gas emissions can be reduced by utilizing aquifers as an energy sink or source for cooling and heating of buildings (Abdel-Salam and Zaidi 2021; Beernink et al. 2022).

Open-loop geothermal systems with proper design can use groundwater directly to reduce indoor temperatures without mechanical cooling by a heat pump. This approach, referred to as “free cooling”, “direct cooling”, “radiant cooling”, or “passive cooling”, offers additional benefits as a result (Fidorów-Kaprawy and Stefaniak 2022; Ünlü et al. 2019). For instance, an ATES system implemented at a municipal hospital in Karlsruhe, Germany, achieved direct cooling that reduced electricity costs by 80% compared to conventional compression chillers. Moreover, the system demonstrated significant environmental benefits, including annual CO_2 reduction of approximately 600 tons (Schüppler et al. 2019). Despite the numerous benefits of free cooling systems, they are not as commonly used as mechanical cooling systems mainly due to challenges related to condensation, cooling capacity limited by temperature differences between the chilled fluid and the indoor air, and potential ventilation issues (Teufl et al., 2021).

Existing research on open-loop geothermal systems has primarily explored aspects such as system performance and environmental impacts from a field and numerical perspective, demonstrating substantial energy savings and reductions in carbon emissions (Ferguson and Woodbury 2006; Sommer et al. 2014; Boon et al. 2019; Ünlü et al. 2019). However, numerical modeling and long-term field monitoring by Boon et al. (2019) have shown that thermal plume dynamics can significantly influence system performance, with potential temperature changes around production wells ranging from 2-4°C. In particular, Ferguson & Woodbury's (2006) study in Winnipeg highlighted sustainability challenges in open-loop geothermal systems, emphasizing the need for site-specific investigations that can address local geological and thermal properties and characteristics. There is, however, a need for more numerical studies to compare the performance of free cooling with that of heat pumps, highlighting benefits to motivate engineering studies tackling the aforementioned technical challenges.

Also, relatively few studies have investigated how open-loop geothermal systems can mitigate the UHI effect. Schibuola and Tambani (2022) demonstrated with a case study in Treviso, Italy, that GWHPs used on a large scale could reduce UHI intensity by 45%, provide 27% energy savings, and achieve a 39.5% CO_2 emissions reduction compared to conventional air conditioning systems. Studies on the performance benefits of free cooling open-loop geothermal systems have also revealed that well spacing critically impact system efficiency, which can be a challenge in an urban setting (Schüppler et al. 2019; Beernink et al. 2022). While previous work on open-loop geothermal systems and free cooling have extensively investigated their performance and environmental impact, none has comprehensively analyzed their potential for UHI mitigation through a comparative approach of multiple system types and configurations.

To address this knowledge gap, the objective of this study was to evaluate and compare GWHP and ATES system performance and thermal impact with and without a free cooling operation mode. A case study was conducted for a well-characterized sandy aquifer in Quebec City (eastern Canada). This Canadian urban context is ideal for space cooling because of the relatively low ground temperature all year long and warm air temperature during summer. Numerical finite element modeling was used to simulate scenarios replicating the conditions of this aquifer with different open-loop geothermal system types and configurations to evaluate their respective performance and impact. One of the goals was to assess whether the free cooling mode is well suited to a Canadian urban context experiencing UHI problems, since it implies a substantial reduction in energy consumption.

2 DESCRIPTION OF THE STUDY SITE

The targeted aquifer covers most of the Lower town of Quebec City. The site, on boulevard Saint-Anne in d'Estimauville, was selected in collaboration with the town administration (Figure1). The granular aquifer is up to 35 m thick and is mainly composed of fine to medium sand. Fieldwork at this site involved the drilling of one injection well and one pumping well of 152 mm (6 in) diameter using a rotary drill rig, and five observation wells (piezometers) of 40 mm (2 in) diameter using a geotechnical rig, from which soil samples were collected and permeability tests performed using compressed air. Most wells are 30 to 32 m deep and were completed just above a clay layer that overlies bedrock in this area. Five (5) meter screens were installed at the bottom portion where there is a gravel dominant unit, except for one monitoring well that was fully screened. Grain-size analyses were carried out on 25 soil samples collected during the drilling of two of the wells. The mean groundwater temperature is about 11°C. Thermal response tests (TRT) using heating cables were conducted to evaluate the ground thermal conductivity in saturated conditions. Twenty-six (26) temperature probes were used in

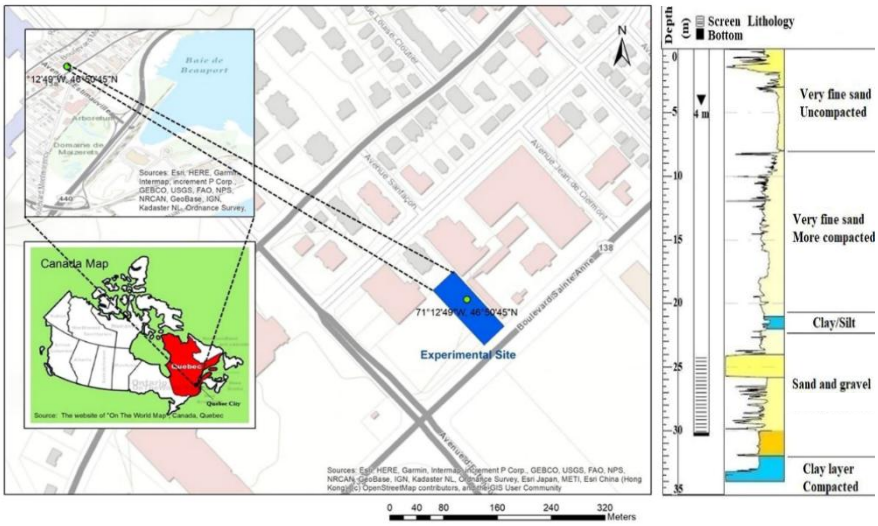


Figure 1. Location of the study site in Quebec City (Quebec, Canada), along with a lithological log of one of the observation wells with a diagram of the installed casing and screen (taken from Shariatinik et al., 2024).

the first TRT along the almost fully screened well (~31 m deep) and 25 for the second well (~32 m deep), which has a screen of only 6 m at the bottom. Temperature measurements were recorded every minute during the heat injection that lasted for approximately 3 days, and for the following 2 days during the thermal recovery. The TRT aimed to provide the effective thermal conductivity of the bulk saturated porous medium. The results obtained for thermal and hydraulic properties and the values retained for models are reported below in the methodology section as they are model inputs (section 3.2.3).

3 METHODOLOGY

The archetype building used to estimate the cooling and heating loads required for the numerical simulations to study open-loop geothermal system performance and thermal impact for the study site is first presented. Methods to calculate system coefficients of performance (COP) and the injection temperature for the comparison between GWHP and ATES systems, as well as free cooling scenarios, are then defined. Finally, the development of a finite element groundwater flow and heat transfer model in FEFLOW is briefly presented. Detailed model development is described in Lee (2025).

3.1 Building Energy Load Assessment, Injection Temperature and System Performance

The program EnergyPlus was used for calculating the cooling and heating loads for the numerical simulations. An example file of an archetype building provided by the American Society of Heating, Refrigeration and Air-Conditioning Engineers in the software's database served as input for the calculations. The large office archetype building, with a total area of 46,320 m^2 across 4 levels (1 basement and 3 above-ground floors) and a maximum occupancy of 724 people, was chosen for the simulations based on the types of existing buildings near the study site. Quebec City weather data were used to determine the hourly cooling and heating loads. A cap was applied for both the cooling and heating loads to balance the distribution of power demand and ground load during the year (Figure 2). The capped values (55% and 17% of the peak monthly average power demand for the cooling and heating seasons, respectively) were determined based on the cooling and heating capacities of the chosen heat pump model and, consequently, on the estimated required energy loads. The modeled geothermal system is assumed to be used to supply base load, while auxiliary systems would be needed to supply the rest of the loads.

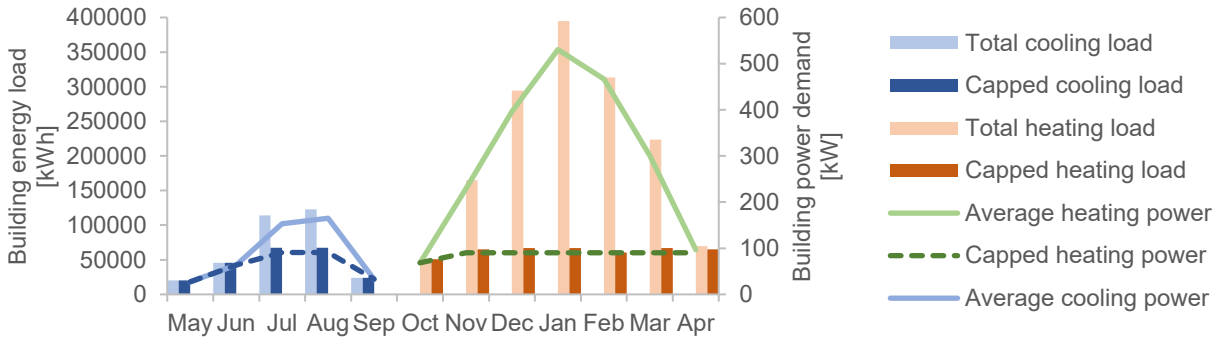


Figure 2. Space cooling and heating energy loads, and power demand for a large office in Quebec City.

Equations were implemented in Python to calculate the injection temperature of the system from the simulated pumping temperature. For modeling scenarios involving heat pumps, a water-to-air geothermal heat pump model from the "WaterFurnace" manufacturer was chosen as the system for the model due to its appropriate cooling and heating capacity. The heat pump model VERSATEC 500 7-30 TON, type 180 - Full Load Horizontal (5200 CFM) with a flow rate of 185.33 m^3/d was selected. Two of these heat pumps are required to meet the capped building demand, so the total flow rate for the system is 370.67 m^3/d.

Based on common efficiency values found for commercial plate heat exchangers, the temperature difference between groundwater and the heat carrier fluid entering the heat pump was assumed to be 3°C. Therefore, this value was added or subtracted to the simulated abstraction well temperature depending on the season (cooling or heating) when calculating the COP. To calculate the well injection temperature in scenarios with no free cooling, Equation 1 was used for the cooling periods and Equation 2 for the heating periods:

$$T_{\mathrm{inj}} = T_{\mathrm{abs}} + \left[\left(\frac{Q_{\mathrm{building}}}{Q \times \rho_{\mathrm{w}} \times c_{\mathrm{w}}}\right) \times \left(\frac{COP_{\mathrm{hp}}+1}{COP_{\mathrm{hp}}}\right)\right] \quad (1)$$

$$T_{\mathrm{inj}} = T_{\mathrm{abs}} - \left[\left(\frac{Q_{\mathrm{building}}}{Q \times \rho_{\mathrm{w}} \times c_{\mathrm{w}}}\right) \times \left(\frac{COP_{\mathrm{hp}}-1}{COP_{\mathrm{hp}}}\right)\right] \quad (2)$$

where T_{inj} [°C] is the injection temperature, T_{abs} [°C] is the abstraction temperature, $Q_{building}$ [kW] is the building load, Q [m^3/s] is the well flow rate, ρ_w [kg/m^3] is the density of water, c_w [kJ/kg °C] is the specific heat capacity of water, and COP_{hp} is the coefficient of performance of the heat pump. For scenarios with 100% free cooling, an efficiency of 90% was assumed for this mode and Equation 3.3 was used to calculate the injection temperature during cooling periods:

$$T_{\text{inj}} = T_{\text{abs}} + \left[\left(\frac{Q_{\text{building}}}{Q \times \rho_{\text{w}} \times c_{\text{w}}}\right) \times 1.1\right] \quad (3)$$

To assess the overall system performance to compare systems with and without free cooling modes, Equations 4 and 5 were used:

$$P_{\text{sp}} = \frac{\rho_{\text{w}} \times g \times Q \times H}{\eta} \quad (4)$$

$$COP_{\text{system}} = \frac{Q_{\text{building}}}{(P_{\text{hp}} + P_{\text{sp}})} \quad \text{and} \quad P_{\text{hp}} = \frac{Q_{\text{building}}}{COP_{\text{hp}}} \quad (5)$$

where P_{sp} and P_{hp} [kW] are the required power of the submersible pump and the system heat pump (not applicable in free cooling mode), respectively, g [m/s^2] is the gravitational acceleration, H [m] is the delivery head equivalent to the well depth added to the building height for free cooling mode, η is the submersible pump efficiency set at 60% (Liang & Fleming, 2012), and COP_{system} is the coefficient of performance of the whole system also considered as the seasonal performance factor (SPF).

3.2 Numerical Model Development

3.2.1 Conceptual Models

2D conceptual models were developed based on the stratigraphy observed at the study site. The first conceptual model (Figure 3) has a GWHP system where the abstraction and pumping wells have constant flow rates and are aligned along the regional groundwater flow direction. The second conceptual model (not shown) is similar to that of Figure 3, but has an ATES system that changes pumping/injection direction depending on the season so that thermal energy is stored in the aquifer, and the wells are aligned perpendicular to the regional groundwater flow direction. The figure for this conceptual model is available in Lee (2025).

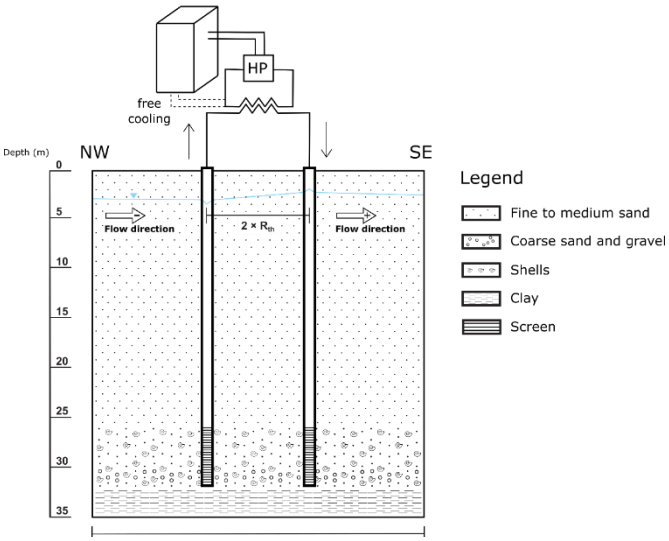


Figure 3. Conceptual model of the GWHP system type (not to scale). R_{th} = Thermal radius to avoid thermal short-circuiting. The two wells are aligned with the groundwater flow direction.

FEFLOW software was used to develop the numerical models and simulate the operation scenarios. The Richards equation for variably saturated flow in unconfined aquifers was selected for the groundwater flow simulation. Heat transport simulations considered advection, conduction and storage, based on Darcy's fluxes obtained from the flow simulation results.

3.2.2 Dimensions, Mesh and Well Spacing

The selected 3D model dimensions are 1400 m × 700 m × 100 m, hence much larger than the conceptual model, to avoid boundary effects and to fully capture the extent of the heat plume. The depth of 100 m (along the z-axis) is divided into 50 layers where the top 40 m is more refined than the bottom. This is because the well depth is 32 m, and less refinement is needed in the aquitard below the aquifer where flow velocity and interaction with the geothermal system are limited.

To decide on an appropriate number of finite elements for the model mesh, four simulations were completed to assess the mesh sensitivity. A 14 000-element mesh was selected because the difference in the model response with the 28 000-element mesh is small enough to be considered acceptable, while the mesh is coarse enough to allow for a reasonable execution time.

To determine the appropriate well spacing, and prevent thermal short-circuiting (where the injection thermal plume reaches the abstraction well), the thermal radius of injection was estimated using an equation proposed by Sommer et al. (2014). The separation distance between wells (110 m) was calculated by multiplying the thermal radius by 2. For the GWHP scenarios, the pumping well was placed 100 m from the edge of the model, and for ATES scenarios, both wells were 150 m away from the edges.

3.2.3 Properties, Boundary and Initial Conditions

The values of all model properties used as inputs for the base case scenarios for flow and heat transport simulations are summarized in Table 1. These include the values obtained from the field assessment of thermal and hydraulic properties described in Section 2. Input values for the various parameters used for the sensitivity analysis (hydraulic conductivity, well spacing and horizontal hydraulic gradient) are presented in Table 2.

Table 1. Input hydraulic and thermal properties for the numerical model.

Stratigraphy		Kx, Ky (m/s)	Kz (m/s)	Effective porosity	Thermal conductivity of solids (W/m*K)
0-26 m	Fine to medium sand	7.05E-05	7.05E-06	0.28	1.46
26-28 m	Medium sand	8.66E-05	8.66E-06	0.32	1.46
28-30 m	Coarse sand with finer interbeds and shells	2.31E-04	2.31E-05	0.3	1.46
30-32 m	Gravel, coarse sand, and shells	3.26E-04	3.26E-05	0.28	1.46
32-60 m	Clay	3.00E-07	3.00E-08	0.02	1.1
60-70 m	Silt	2.00E-07	2.00E-08	0.08	1.1
70-100 m	Shale	5.00E-07	5.00E-08	0.03	1.1

Inputs applied to entire model	
Specific storage	0.0001 m^{-1}
Volumetric heat capacity of fluid	4.2 J/m^3*K
Volumetric heat capacity of solid	2.52 J/m^3*K
Thermal conductivity of fluid	0.65 W/m*K

Table 2. Model input parameters according to their respective modeling scenario.

	Base case	100% free cooling	Kmax	½ X well spacing	1/10 X gradient
Free cooling	0%	100%	0%	0%	0%
Hydraulic conductivity (x,y)					
0-26 m	7.05E-5 m/s	7.05E-5 m/s	1.62E-4 m/s	7.05E-5 m/s	7.05E-5 m/s
26-28 m	8.66E-5 m/s	8.66E-5 m/s	2.18E-4 m/s	8.66E-5 m/s	8.66E-5 m/s
28-30 m	2.31E-4 m/s	2.31E-4 m/s	1.77E-2 m/s	2.31E-4 m/s	2.31E-4 m/s
30-32 m	3.26E-4 m/s	3.26E-4 m/s	2.79E-2 m/s	3.26E-4 m/s	3.26E-4 m/s
32-60 m	3E-7 m/s	3E-7 m/s	3E-7 m/s	3E-7 m/s	3E-7 m/s
60-70 m	2E-7 m/s	2E-7 m/s	2E-7 m/s	2E-7 m/s	2E-7 m/s
70-100 m	5E-7m/s	5E-7m/s	5E-7 m/s	5E-7m/s	5E-7m/s
Hydraulic conductivity (z)					
0-26 m	7.05E-6 m/s	7.05E-6 m/s	1.62E-5 m/s	7.05E-6 m/s	7.05E-6 m/s
26-28 m	8.66E-6 m/s	8.66E-6 m/s	2.18E-5 m/s	8.66E-6 m/s	8.66E-6 m/s
28-30 m	2.31E-5 m/s	2.31E-5 m/s	1.77E-3 m/s	2.31E-5 m/s	2.31E-5 m/s
30-32 m	3.26E-5 m/s	3.26E-5 m/s	2.79E-3 m/s	3.26E-5 m/s	3.26E-5 m/s
32-60 m	3E-8 m/s	3E-8 m/s	3E-8 m/s	3E-8 m/s	3E-8 m/s
60-70 m	2E-8 m/s	2E-8 m/s	2E-8 m/s	2E-8 m/s	2E-8 m/s
70-100 m	5E-8 m/s	5E-8 m/s	5E-8 m/s	5E-8 m/s	5E-8 m/s
Well spacing	110 m	110 m	110 m	55 m	110 m
Hydraulic gradient (i)	8 mm/m	8 mm/m	8 mm/m	8 mm/m	0.8 mm/m

The boundary conditions for both the GWHP and ATES systems are based on data from fieldwork, including direct temperature and water-level measurements, and from literature for the average annual recharge value, found to be 200 mm/y (Talbot Poulin et al., 2013). Vertical recharge was applied to the top boundary and was assumed to have the same temperature as the groundwater. Constant head conditions were applied on the western and eastern boundaries to impose the estimated hydraulic gradient. A fixed temperature condition was assigned to the western boundary, where groundwater at the study site originates. The bottom and lateral boundaries (i.e. aligned with groundwater flow direction) are defined as no-flow conditions.

The initial conditions for the hydraulic head values across the model domain were obtained using a steady state simulation to represent the aquifer flow conditions before pumping and injection. As for the initial temperature, the same value as the fixed temperature boundary conditions was applied to the entire model (11°C).

The Python code developed by Gascuel et al. (2024) was used to calculate the injection temperature, which is dependent on the pumped groundwater temperature and building energy load changing through time. This temperature was applied as a "Temperature BC" at each time step for each node along the well screen.

The simulation time for all scenarios was set to 25 years because it represents a realistic lifespan of a GWHP or ATES system. The length of the time steps was determined automatically by the modeling software to ensure convergence of the solution.

4 RESULTS

This section is structured based on the following three groupings of scenarios: base case scenarios, sensitivity analysis of key parameters and free cooling impact. Within these groupings, system performance and system thermal impact results are presented. Additional details and figures are available in Lee (2025).

4.1 Base Case Scenarios

COP values for the GWHP simulations were shown to be stable throughout the two different periods (around 4.93 for the cooling period and 3.63 for the heating period), while those for the ATES decrease almost continuously from 5.17 at the beginning of the cooling period to 3.65 at the end of the heating period. The SPF values at the end of the simulation period, which consider the energy required for the operation of the heat pumps and the submersible pump, are significantly better for the cooling (4.26 and 4.18) than the heating (3.33 and 3.37) periods for both system types (Figure 4).

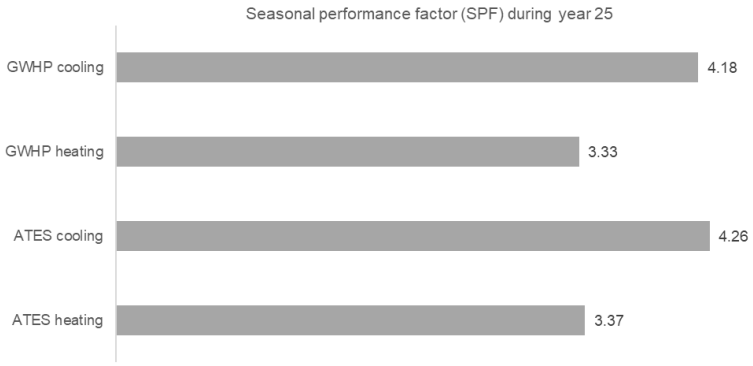


Figure 4. SPF during the cooling and heating periods of the last simulation year (year 25) for GWHP and ATES base case scenarios.

The temperature impact at the end of the last cooling and heating periods (year 25) for both GWHP and ATES system simulations are evaluated using the size of the thermal plume (Figure 5). The aquifer undisturbed temperature is 11℃ and the measured width and length represent the extent of groundwater at 12℃ and 10℃ for the cooling and heating periods, respectively. While plumes for the cooling period from both types of systems for the 1°C difference are relatively similar, the plume for the heating period for the ATES system is significantly longer (~2.5 times). This is not surprising since groundwater flow is perpendicular to the well alignment for the ATES scenarios.

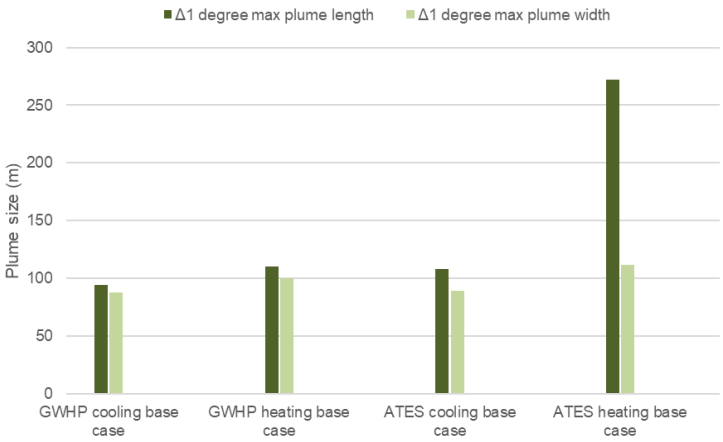


Figure 5. The 1°C difference plume sizes in the last simulation year (year 25) for the GWHP and ATES base case

4.2 Sensitivity Analysis of Key Parameters

Simulation scenarios of Table 2 were compared in order to evaluate the influence of key parameters on the performance of the open-loop geothermal systems. All scenarios have the same well flow rate, and the pumping well drawdown is around 3.7 m.

The COP curves determined from pumped water for all simulations have relatively the same behavior as the base case, except for the scenario where half of the well spacing is used. In the latter, a nearly continuous decrease of the COP suggests that thermal short-circuiting has occurred for the GWHP system. COP values are, however, all quite close, decreasing from 5.2 to 4.9 for the cooling period and from 3.7 to 3.6 for the heating period, with the highest values obtained with the ATES system.

All SPF values for the scenarios studied (Table 2), for a given cooling/heating season and system type, are also similar (variations are within 5%). Nonetheless, some differences can be noted. For GWHP systems, the best SPF value (4.20) was found with both the 1/10× hydraulic gradient and 1/2× smaller well distance scenarios during the cooling period, and the worst SPF value (3.31) was found with the 1/10× hydraulic gradient scenario as well, but during the heating period. ATES systems, on the other hand, had the best overall SPF value (4.30), which was found with the 1/10× hydraulic gradient scenario during the cooling period, while their worst SPF value (3.33) was found with the Kmax scenario during the heating period, mainly because the stored energy dissipated too quickly.

The change in hydraulic conductivity values (Kmax scenario) significantly influences the thermal impact compared to the base case and increases by a factor of 1.5 to 2 the plume length for the GWHP system during both cooling and heating periods. The complete opposite occurs for the ATES system during the cooling and heating periods, as the increase in hydraulic conductivity reduces the plume size to less than 5 m (both in length and width), because the heat is easily dissipated. Plume images for all simulation scenarios are available in Lee (2025).

4.3 Free Cooling Impact

Compared to the base case scenario, the performance of the 100% free cooling scenario (Table 2) during the cooling period is much higher (SPF of 19.13) and remains essentially the same as that of the base case during the heating period (Figure 6). This demonstrates that very high performance can be achieved with a free cooling system without compromising the performance of the heat pump used during winter for heating.

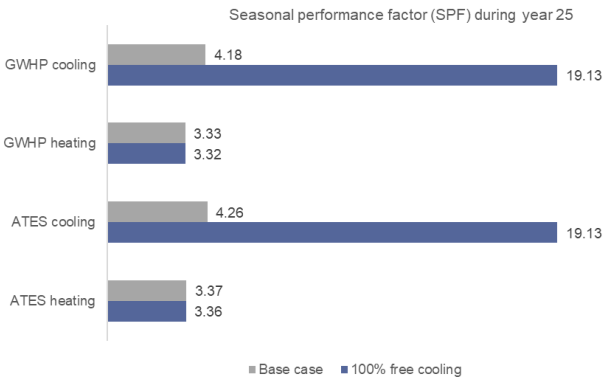


Figure 6. SPF during the cooling and heating periods of the last simulation year (year 25) for the base case and 100% free cooling GWHP and ATES scenarios.

In three out of the four cases simulated with and without free cooling, the differences in plume size are minimal (see Lee (2025) for images of the plume). This confirms that the thermal impact of 100% free cooling on the aquifer is not significant in comparison with the base case. Nonetheless, the plume length for the ATES system with free cooling is about 10% longer than the base case scenario during the heating period, but this does not seem to affect the system performance (Figure 6).

These results can be attributed to the way free cooling interacts with the aquifer. Unlike heat pump systems, which reject both the building and compressor heat, free cooling only transfers the extracted building heat, resulting in lower overall heat rejection during the cooling season. While this can reduce the thermal impact on the aquifer in summer, it also means less heat is stored for recovery in winter although heat pump performance is barely affected.

5 DISCUSSION

The system performance obtained using numerical simulations in this study are comparable to results from other locations with various types of geothermal systems, although specific factors such as aquifer properties and weather conditions differ. Boon et al. (2019) found an SPF of 4.5 for heating for a pilot GWHP system in Cardiff, United Kingdom. Vanhoudt et al. (2011) reported an SPF value of 5.9 for heating and an efficiency factor of 26.1 for cooling for an ATES system in a Belgian hospital. In comparison, this numerical study in Quebec City found SPFs, for heating and cooling, of 3.33 and 4.18 for the GWHP system, and 3.37 and 4.26 for the ATES system, respectively. The differences in performance, for both theoretical and for on-site studies, depend on multiple factors, including climate, system type and design, and operational strategies such as pumping rates.

The assessment of thermal plume dynamics and temperature changes around pumping wells within this study is consistent with the broader literature on thermal interference. Ferguson & Woodbury (2006) highlight potential thermal interference and sustainability challenges in open-loop geothermal systems. They observed rising temperatures at production wells due to injected water breakthrough and noted interference effects between

closely spaced systems in Winnipeg, Canada. Similarly, Sommer et al. (2014) and Bloemendal et al. (2018) emphasize that sufficient well spacing prevents thermal interference, while over sizing well spacing may limit the number of systems that can be installed in an area and lower the effectiveness of ATES. This study's findings, which estimated thermal plume sizes of different open-loop systems and the impact of various parameters such as hydraulic conductivity, hydraulic gradient and well spacing contribute to this understanding by providing quantitative data on these effects for a given hydrogeological setting. The well spacing set at twice the estimated thermal radius was sufficient to maintain good performance.

Integrating a free cooling proportion into open-loop geothermal systems significantly reduces the need for mechanical cooling with heat pumps. In our study, 100% free cooling was simulated and yielded a very high SPF value of 19.13 during cooling periods, an efficiency gain that directly translates into less waste heat rejected into the urban environment. This reduced heat rejection is critical for mitigating the urban heat island (UHI) effect, as it can help to maintain lower ambient temperatures in densely built areas.

When compared with other free cooling technologies that have demonstrated significant energy savings, such as high-temperature radiant systems supplied by ground heat exchangers (Fidorów-Kaprawy & Stefaniak, 2022; Pieskä et al., 2022a and b), our results suggest that integrating free cooling with open-loop geothermal systems can provide comparable, if not superior, performance. Pieskä et al. (2022a) have demonstrated that integrating free cooling technologies with geothermal systems can substantially reduce compressor energy demand while improving thermal comfort by providing steady, moderate temperatures.

From a practical perspective, these findings support the feasibility and relevance of integrating open-loop geothermal and free cooling into urban planning to combat UHI. Canadian cities, with their relatively low groundwater temperatures and the often-favorable properties of the underlying geological units (Lee, 2025), appear well suited for such systems. UHIs are caused in part by the absorption and retention of heat in built environments, especially through impervious surfaces and waste heat rejection from heating, ventilating and air conditioning systems (Oke 1982; Santamouris et al. 2015). One contributor to UHIs is the release of heat into the urban atmosphere during summer cooling, particularly by conventional air conditioning systems. In contrast, open-loop geothermal systems, reject excess heat into the subsurface rather than the air, thereby limiting the direct thermal discharge on the urban environment, especially when operating in free cooling mode.

While this numerical study provides valuable insights into the performance and potential of GWHP and ATES systems with free cooling in Quebec City, several constraints and limitations must be acknowledged, some of which are well documented in the literature, and others remain specific to conditions of our study site. A primary concern is the potential for aquifer thermal accumulation, particularly with operating ATES systems. Long-term imbalances between heat injection and extraction can lead to gradual warming or cooling of the aquifer, which could negatively impact system performance and potentially affect groundwater quality (Possemiers et al. 2014). In our study, the simulated plume for the ATES system was 2.5 times longer compared to GWHP systems for the heating period. As Bonte et al. (2014) and Vienken et al. (2019) point out, a lack of comprehensive long-term in situ data creates uncertainty about the ecological impact and economic implications of open-loop systems over their full operational lifespan. This uncertainty needs to be addressed through continued monitoring, research, and adaptive management strategies. Balancing heat supply and energy extraction, as well as maintaining groundwater temperature to keep the system efficient, are critical aspects to consider (Wu et al. 2015). In this study, heat loads were balanced by applying a cap to both cooling and heating demands, ensuring a more stable average groundwater temperature over time.

This study was subject to certain methodological constraints. Numerical modeling relied on important simplifying assumptions, including the homogeneity and continuity of aquifer units and a fixed ratio for anisotropic conditions. Also, energy consumption for ventilation and dehumidification was not considered in the performance calculations for free cooling systems, and friction losses were not considered in total delivery head calculations for the circulation pump. The UHI effect was not fully considered either, because the building energy demand calculations rely on climatic data recorded at an airport station outside downtown Quebec City, although the UHI effect was considered for the groundwater temperature. This can be detrimental to the cooling performance (but beneficial to the heating performance) because urban groundwater systems are often thermally increased due to the subsurface UHI effect, and shallow groundwater temperatures usually slightly exceed the average annual air temperature during this period (Farr et al. 2017).

6 CONCLUSIONS

This study numerically investigated the performance and thermal impact of GWHP and ATES systems in Quebec City, Canada, both with a free cooling option, to assess their potential for UHI mitigation in an urban environment

with a cold climate (winter). Various scenarios were simulated to evaluate system performance and impact on the aquifer's thermal behavior. One of the objectives was to determine if free cooling is well suited for a Canadian urban context given its major advantage to reduce the energy required to space conditioning.

This study showed that both GWHP and ATES systems can efficiently cool urban spaces in a cold Canadian climate, with free cooling playing a key role in enhancing performance. Key findings for our simulations in Quebec City include:

- ATES systems overall performed slightly better than GWHP systems due to more efficient abstraction temperatures from stored thermal energy.
- Temperature plumes for the heating period were significantly longer (up to 164 m, i.e. 2.5 times) than those for the cooling period in ATES scenarios, as expected.
- Changes in hydraulic conductivity significantly impacted the extent of thermal plumes.
- 100% free cooling resulted in higher performance during the cooling period, with an SPF of 19.13 for both system types, while maintaining virtually the same for GWHP (3.32 versus 3.33) and for ATES (3.36 versus 3.37) during the heating period.
- The thermal impact of 100% free cooling on the aquifer was not significant compared to the base case.

Overall, the results demonstrate that both GWHP and ATES systems can achieve efficient cooling performance, with ATES systems benefiting from stored thermal energy and free cooling significantly enhancing system efficiency without causing adverse thermal impacts on the aquifer. We hope that results presented will facilitate engineering studies and other in situ tests to better understand the operating conditions of geothermal heat pump systems that can help mitigate UHI effects.

Acknowledgements

This work was funded by a grant awarded to INRS under the Advancing Climate Change Science in Canada program of the Natural Sciences and Engineering Research Council (NSERC) of Canada. The first author was also funded by a Canada Graduate Scholarship from NSERC for her master's program.

REFERENCES

Abdel-Salam, M.R.H. and Zaidi, A.: Field study of cooling performance of two ground-source heat pumps in Canadian single-family houses. *Applied Thermal Engineering*, **184**, (2021), 116294, https://doi.org/10.1016/j.applthermaleng.2020.116294.

Beernink, S., Bloemendal, M., Kleinlugtenbelt, R. and Hartog, N.: Maximizing the use of aquifer thermal energy storage systems in urban areas: effects on individual system primary energy use and overall GHG emissions. *Applied Energy*, **311**, (2022), 118587, https://doi.org/10.1016/j.apenergy.2022.118587.

Bloemendal, M., Jaxa-Rozen, M. and Olsthoorn, T.: Methods for planning of ATES systems. *Applied Energy*, **216**, (2018), 534–557, https://doi.org/10.1016/j.apenergy.2018.02.068.

Bonte, M., Stuyfzand, P.J. and Breukelen, B.M. van.: Reactive Transport Modeling of Thermal Column Experiments to Investigate the Impacts of Aquifer Thermal Energy Storage on Groundwater Quality. *Environmental Science & Technology*, **48**, (2014), 12099–12107, https://doi.org/10.1021/es502477m.

Boon, D.P., Farr, G.J., Abesser, C., Patton, A.M., James, D.R., Schofield, D.I. and Tucker, D.G.: Groundwater heat pump feasibility in shallow urban aquifers: Experience from Cardiff, UK. *Science of The Total Environment*, **697**, (2019), 133847, https://doi.org/10.1016/j.scitotenv.2019.133847.

Farr, G.J., Patton, A.M., Boon, D.P., James, D.R., Williams, B. and Schofield, D.I.: Mapping shallow urban groundwater temperatures, a case study from Cardiff, UK. *Quarterly Journal of Engineering Geology and Hydrogeology*, **50**, (2017), 187–198, https://doi.org/10.1144/qjegh2016-058.

Ferguson, G. and Woodbury, A.: Observed thermal pollution and post-development simulations of low-temperature geothermal systems in Winnipeg, Canada. *Hydrogeology Journal*, **14**, (2006), 1206–1215, https://doi.org/10.1007/s10040-006-0047-y.

Fidorów-Kaprawy, N. and Stefaniak, Ł.: Potential of CO_2 Emission Reduction via Application of Geothermal Heat Exchanger and Passive Cooling in Residential Sector under Polish Climatic Conditions. *Energies*, **15**, (2022), 8531, https://doi.org/10.3390/en15228531.

Gascuel, V., Rivard, C. and Raymond, J.: Deep geothermal doublets versus deep borehole heat exchangers: A comparative study for cold sedimentary basins. *Applied Energy*, **361**, (2024), 122826, https://doi.org/10.1016/j.apenergy.2024.122826.

Lee, V.: *Lutter contre les îlots de chaleur urbain : évaluation du potentiel des systèmes de pompe à chaleur géothermique à boucle ouverte au Canada*. Master Thesis, Institut national de la recherche scientifique, Quebec City, Canada (2025).

Oke, T.R.: The energetic basis of the urban heat island. Q*uarterly Journal of the Royal Meteorological Society*, **108**, (1982), 1–24, https://doi.org/10.1002/qj.49710845502.

Pieskä, H., Ploskić, A., Holmberg, S. and Wang, Q.: Performance Analysis of a Geothermal Radiant Cooling System Supported by Dehumidification. *Energies*, **15**, (2022a), 2815, https://doi.org/10.3390/en15082815.

Pieskä, H., Wang, C., Nourozi, B., Ploskić, A. and Wang, Q.: Thermodynamic and thermal comfort performance evaluation of two geothermal high-temperature cooling systems in the mediterranean climate. *Journal of Building Engineering*, **56**, (2022b), 104738, https://doi.org/10.1016/j.jobe.2022.104738.

Possemiers, M., Huysmans, M. and Batelaan, O.: Influence of Aquifer Thermal Energy Storage on groundwater quality: A review illustrated by seven case studies from Belgium. *Journal of Hydrology: Regional Studies*, **2**, (2014), 20–34, https://doi.org/10.1016/j.ejrh.2014.08.001.

Salamanca, F., Georgescu, M., Mahalov, A., Moustaoui, M. and Wang, M.: Anthropogenic heating of the urban environment due to air conditioning. *Journal of Geophysical Research: Atmospheres*, **119**, (2014), 5949–5965, https://doi.org/10.1002/2013JD021225.

Santamouris, M., Cartalis, C., Synnefa, A. and Kolokotsa, D.: On the impact of urban heat island and global warming on the power demand and electricity consumption of buildings—A review. *Energy and Buildings*, **98**, (2015), 119–124, https://doi.org/10.1016/j.enbuild.2014.09.052.

Schüppler, S., Fleuchaus, P. and Blum, P.: Techno-economic and environmental analysis of an Aquifer Thermal Energy Storage (ATES) in Germany. *Geothermal Energy*, **7**, (2019), 11, https://doi.org/10.1186/s40517-019-0127-6.

Shariatinik, B., Gloaguen, E., Raymond, J., Boutin, L.-C. and Fabien-Ouellet, G.: ERT data assimilation to characterize aquifer hydraulic conductivity heterogeneity through a heat-tracing experiment. *Near Surface Geophysics*, **22**, (2024), 358–371, https://doi.org/10.1002/nsg.12288.

Sommer, W.T., Doornenbal, P.J., Drijver, B.C., van Gaans, P.F.M., Leusbrock, I., Grotenhuis, J.T.C. and Rijnaarts, H.H.M.: Thermal performance and heat transport in aquifer thermal energy storage. *Hydrogeology Journal*, **22**, (2014), 263–279, https://doi.org/10.1007/s10040-013-1066-0.

Talbot Poulin, M.C., Comeau, G., and Tremblay, Y., Therrien, R., Nadeau, M.M., Lemieux, J.M., Molson, J., Fortier, R., Therrien, P., Lamarche, L., Donati-Daoust, F., Bérubé, S.: Projet d'acquisition de connaissances sur les eaux souterraines du territoire de la communauté métropolitaine de Québec, Rapport Final, Université Laval, Québec, Canada, (2013).

Ünlü, A., Carus, E. and Görgülü, A.: Water Heat Pump Application With Double Stage Back Injection. *Procedia Computer Science*, **158**, (2019), 68–73, https://doi.org/10.1016/j.procs.2019.09.028.

Vanhoudt, D., Desmedt, J., Van Bael, J., Robeyn, N. and Hoes, H.: An aquifer thermal storage system in a Belgian hospital: Long-term experimental evaluation of energy and cost savings. *Energy and Buildings*, **43**, (2011), 3657–3665, https://doi.org/10.1016/j.enbuild.2011.09.040.

Vienken, T., Kreck, M. and Dietrich, P.: Monitoring the impact of intensive shallow geothermal energy use on groundwater temperatures in a residential neighborhood. *Geothermal Energy*, **7**, (2019), 8, https://doi.org/10.1186/s40517-019-0123-x.

Vujovic, S., Haddad, B., Karaky, H., Sebaibi, N. and Boutouil, M.: Urban Heat Island: Causes, Consequences, and Mitigation Measures with Emphasis on Reflective and Permeable Pavements. *CivilEng*, **2**, (2021), 459–484, https://doi.org/10.3390/civileng2020026.

Wu, Q., Xu, S., Zhou, W. and LaMoreaux, J.: Hydrogeology and design of groundwater heat pump systems. *Environmental Earth Sciences*, **73**, (2015), 3683–3695, https://doi.org/10.1007/s12665-014-3654-2.